Available online at www.sciencedirect.com
SCIENCE DIRECT®
Journal of Power Sources 140 (2005) 381–387
JOURNAL OF POWER SOURCES
www.elsevier.com/locate/jpowsour

Effect of substituting Mm with La on the electrochemical performances of Co-free $La_xMm_{1-x}(NiMnSiAlFe)_{4.9}$ (x = 0–1) electrode alloys prepared by casting and rapid quenching

Yang-huan Zhang[a,b,*], Xiao-ping Dong[b], Guo-qing Wang[a], Shi-hai Guo[a], Xin-lin Wang[a]

[a] *Department of Functional Material Research, Central Iron and Steel Research Institute, Beijing 100081, China*
[b] *School of Material, Inner Mongolia University of Science and Technology, Baotou 014010, China*

Received 21 June 2004; received in revised form 23 August 2004; accepted 23 August 2004
Available online 8 October 2004

Abstract

In order to enhance the electrochemical capacity of the Co-free AB_5-type electrode alloy, Mm in the alloys was substituted with La and Co-free $La_xMm_{1-x}(NiMnSiAlFe)_{4.9}$ (x = 0, 0.45, 0.75, 1.0) hydrogen storage alloys were prepared by casting and rapid quenching. The effects of the substituting Mm with La on the electrochemical performances of the as-cast and quenched alloys were investigated in detail. The obtained results show that substituting Mm with La can enhance markedly the capacities of the as-cast and quenched alloys. When the amount of substituting Mm with La, x increased from 0 to 1.0, the maximum capacity of the as-cast alloys at 0.2C rate increased from 273.45 to 304.47 mAh g^{-1}, and the capacity retaining rate (R_h) increased from 59.16 to 59.86%. The capacity of the as-quenched alloys with a quenching rate of 10 m s^{-1} increased from 236.83 to 300.31 mAh g^{-1}, and the capacity retaining rate (R_h) decreased from 78.69 to 62.29%. The substituting Mm with La had an insignificant effect on the activation capabilities of the as-cast and quenched alloys.

Keywords: Substituting Mm with La; Co-free; AB_5-type hydrogen storage alloy; As-cast and rapidly quenched; Electrochemical performances

1. Introduction

In recent years, the rechargeable Ni-MH cells are encountering serious competition from Li-ion cells since the Li-ion cells show higher energy density than the Ni-MH cells per unit weight or volume. On the other hand, the production cost of Ni-MH battery based on the current hydride technology also limits the widespread applications as power sources of electric vehicles or hybrid cars because low-cost Pb-acid batteries are still dominating over the segment. According to the typical AB_5-type alloy formula, e.g. $MmNi_{3.5}Co_{0.75}Mn_{0.4}Al_{0.3}$, Co content takes up about 10 wt.% and 40–50% share of the total cost of the raw materials. Therefore, researchers have naturally paid much attention on the decrease of Co content in the alloys [1–8], but the function of Co on the cycle stability of AB_5-type hydrogen storage alloy is extremely important [9]. So, the study emphasis is how to enhance electrochemical cycle stability of the low-Co and Co-free hydrogen storage alloys. In order to maintain the satisfactory cycle stability of low-Co or Co-free AB_5-type alloy, a great lot of efforts have been carried out at many laboratories around the world [10–12]. However, the electrochemical cycle stability of the low-Co or Co-free AB_5-type alloy was unsatisfactory [13,14]. The low-Co AB_5-type hydrogen storage alloy with special microstructure composed of microcrystal, nanocrystal and amorphous phase can be prepared by rapid quenching and the alloy thus prepared has an excellent initial activation capability and outstanding electrochemical cycle stability [4,15]. However, rapid solidification generally decreases the discharge capacity [2,16].

* Corresponding author. Tel.: +86 10 62187570; fax: +86 10 62182296.
E-mail addresses: ljlgrace@vip.sina.com, zyh59@yahoo.com.cn (Y.-h. Zhang).

0378-7753/$ – see front matter © 2004 Elsevier B.V. All rights reserved.
doi:10.1016/j.jpowsour.2004.08.025

In order to enhance the capacities of the Co-free AB_5-type $La_xMm_{1-x}(NiMnSiAlFe)_{4.9}$ ($x = 0$–1.0) hydrogen storage alloys prepared by rapid quenching, the different amount of Mm in the alloys was substituted with La. The obtained results indicate that the Co-free AB_5-type hydrogen storage alloy with excellent synthetical electrochemical performances can be prepared by adjusting the amount of the substitution Mm with La and employing appropriate rapid quenching technique.

2. Experimental details

2.1. Alloy preparation

The chemical compositions of the experimental alloys are $La_xMm_{1-x}(NiMnSiAlFe)_{4.9}$ (x = 0, 0.45, 0.75, 1.0). Corresponding with the amount of La substitution x, the alloys are represented with La_0, $La_{0.45}$, $La_{0.75}$, La_1. The purity of all the components (Ni, Mn, Al, Fe, La and Si) is at least 99.7%. Mm denotes Ce-rich Mischmetal (23.70 wt.% La, 55.29 wt.% Ce, 5.31 wt.% Pr, 15.70 wt.% Nd) and its purity is 99.85 wt.%. The experimental alloys were melted in an induction furnace in a argon atmosphere and cooled in a water-cooling copper mould, and the parts of the as-cast alloys were re-melted and quenched by melt-spinning with a rotating copper wheel, obtaining flakes of the as-quenched alloys with the thickness of 20–45 μm. The quenching rates used in the experiment are 10, 16, 22 and 28 m s^{-1}, which is expressed by the linear velocity of the rotating copper wheel.

2.2. Electrode preparation and electrochemical measurement

The alloy samples were mechanically ground into powder below 250 mesh. Electrode pellets (d = 15 mm) were prepared by mixing 1 g alloy powder and 1 g Ni powder as well as a small amount of polyvinyl alcohol (PVA) solution as binder, and then compressed under a pressure of 35 MPa for 5 min. After drying for 4 h, the electrode pellets were immersed in 6M KOH solution for 24 h in order to wet fully the electrodes before the electrochemical measurement. The experimental electrodes were tested in a tri-electrode open cell, consisting of a working electrode (metal hydride electrode), a counter electrode ($Ni(OH)_2$/NiOOH) and a reference electrode (Hg/HgO) and 6 M KOH solution as electrolyte. The voltage between the working electrode and the reference electrode was defined as the discharge voltage. Every cycle was overcharged to about 30% with constant current, resting 15 min and −0.500 V cut-off voltage. The activation performance and the maximum discharge capacity were measured with a current density of 60 mA g^{-1}, and the cycle life with a current density of 300 mA g^{-1}. The environmental temperature of the measurement was kept at 30 °C.

2.3. Microstructure determination and morphology observation

The samples of the as-cast alloys were directly polished, and the flakes of the as-quenched alloys were inlaid in epoxy resin for polishing. The samples thus prepared were etched with a 60% HF solution. The morphologies of the as-cast and quenched alloys were observed by S.E.M. The samples of as-cast and quenched alloys were pulverized by mechanical grinding, and the sizes of the powder samples are less than 50 μm. The phase structures and lattice constants of the as-cast and quenched alloys were detected by XRD, and the type of X-ray diffractometer used in this experiment is D/max/2400. The diffraction was performed with Cu $K\alpha_1$ radiation filtered by graphite. The experimental parameters for determining the phase composition were 160 mA, 40 kV and 10° min^{-1}, respectively. The powder samples were dispersed in anhydrous alcohol for observing grain morphology with TEM, and for determining crystal status of the as-quenched alloys with SAD.

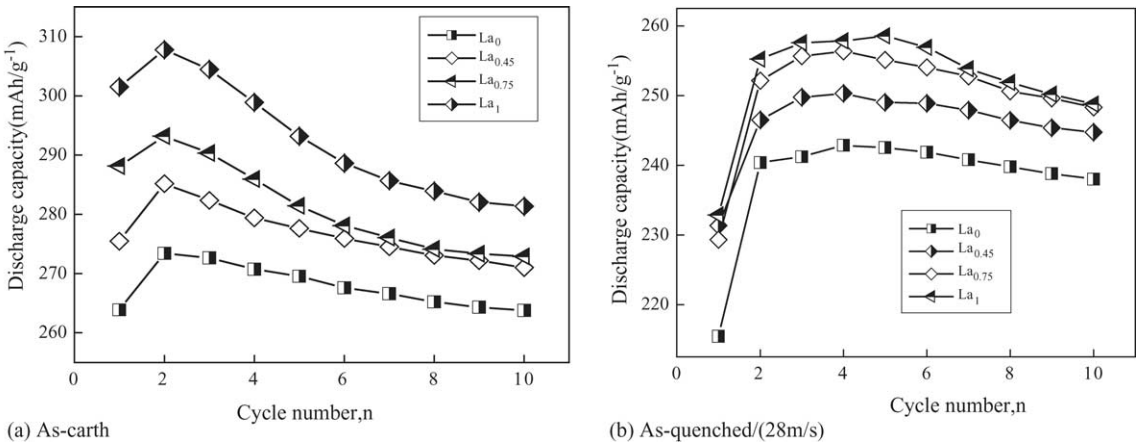

Fig. 1. The relationship between the cycle number and the discharge capacity of the alloys.

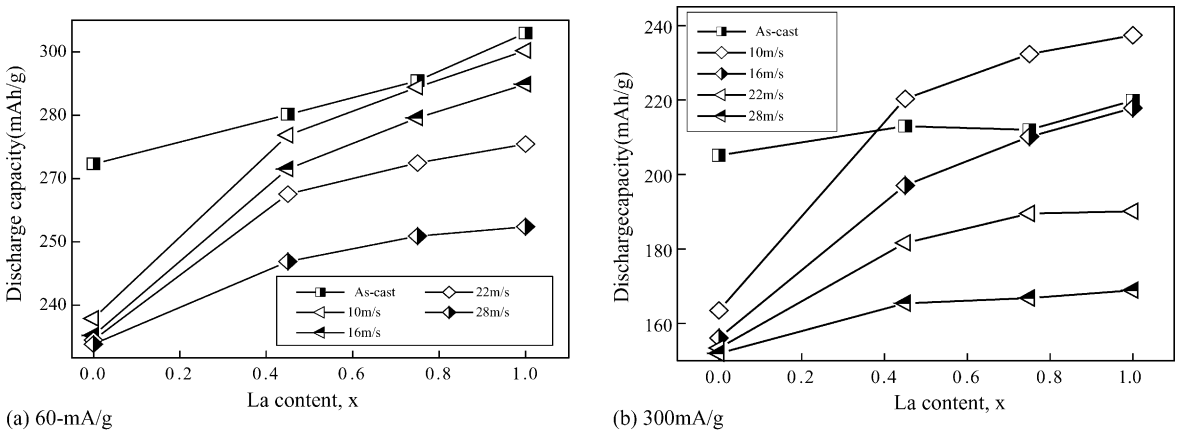

Fig. 2. The relationship between the amount of La substitution and the discharge capacity.

3. Results and discussion

3.1. Effects of substituting Mm with La on the electrochemical performances

3.1.1. Activation performance

The activation capability is characterized by the initial activation number. The initial activation number denoted by n is defined by the number of charge–discharge cycle required for attaining the maximum discharge capacity through a charge–discharge cycle at a constant current. The cycle number dependence of the discharge capacity of the as-cast and quenched alloys with the current density of 60 mA g^{-1} was illustrated Fig. 1. It can be derived from Fig. 1 that substituting Mm with La has an insignificant effect on the activation capabilities of the as-cast and quenched alloys. The as-cast alloys were completely activated through two cycles, and the as-quenched alloys with the quenching rate of 28 m s^{-1} need four cycles to be fully activated.

3.1.2. Discharge capacity

The maximum discharge capacities of the as-cast and quenched alloys were measured with constant current densities of 60 and 300 mA g^{-1}, respectively. The relationship between the amount of substituting Mm with La and the maximum discharge capacities of the as-cast and quenched alloys was illustrated in Fig. 2. Fig. 2 shows that the discharge capacities of the as-cast and quenched alloys increased with the increase of La content with different discharge current densities.

When the amount of the substituting Mm with La, x increased from 0 to 1, the maximum capacities of the as-cast alloys with current density of 60 mA g^{-1} increased from 273.45 to 304.47 mAh g^{-1}, and that of the as-quenched alloy obtained with a quenching rate of 10 m s^{-1} increased from 236.83 to 300.31 mAh g^{-1}. When the discharge current density was 300 mA g^{-1}, the capacities of the as-cast alloys increased from 205.14 to 219.85 mAh g^{-1}, and that of the as-quenched alloy obtained with the quenching rate of 10 m s^{-1} increased from 163.48 to 237.38 mAh g^{-1}.

3.1.3. Cycle life

The capacity retaining rate (R_h), which is introduced to evaluate accurately the cycle stability of the alloy, is defined as $R_h = C_{300,300}/C_{300,max} \times 100\%$, where $C_{300,max}$ is the maximum discharge capacity and $C_{300,300}$ is the discharge capacity of the 300th cycle at 300 mA g^{-1}, respectively.

The La content dependence of the capacity retaining rate of the as-cast and quenched alloys was illustrated in Fig. 3. It can be seen from Fig. 3 that the capacity retaining rates of the as-cast alloys have an almost imperceptibly change with the increase of La content. The capacity retaining rates of the alloys with quenching rates of 22 and 28 m s^{-1} decreased slightly with the increase of La content. However, when the quenching rates are 10 and 16 m s^{-1}, the capacity retaining rates of the alloys decrease significantly with the increase of the amount of substituting Mm with La. The results show that the increase of the La content is unfavourable for the cycle lives of the as-quenched alloys.

3.2. Effect of substitution Mm with La on the phase structure and microstructure

3.2.1. Phase composition and structure

The phase compositions and structures of the as-cast and quenched alloys with the quenching rate of 22 m s^{-1} were

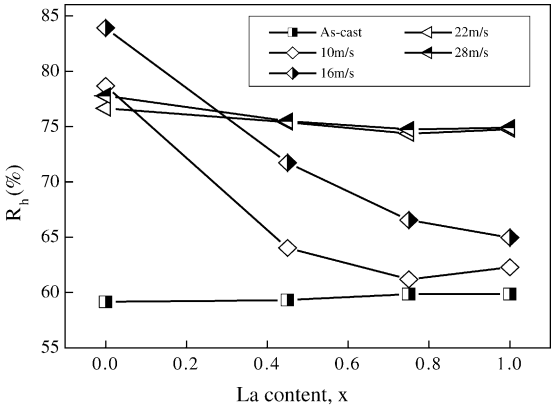

Fig. 3. the relationship between La content and capacity retaining rate (R_h).

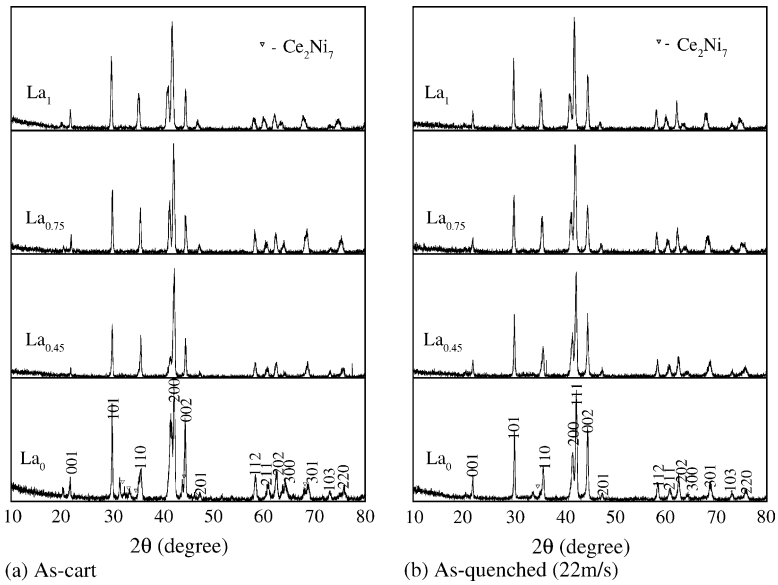

Fig. 4. The X-ray diffraction patterns of the as-cast and quenched alloys.

determined by XRD. The obtained diagrams of the as-cast and quenched alloys were illustrated in Fig. 4. Fig. 4 shows that the as-cast and quenched La_0 alloys have a two-phase structure composed of a $CaCu_5$-type main phase and a small amount of Ce_2Ni_7-type secondary phase, and the presence of the Ce_2Ni_7 phase is because the alloy components are non-stoichiometric. The Ce_2Ni_7-type phase almost disappears with the increase of the amount of substitution Mm with La. This is probably attributed to the decrease of the amount of Ce content in the alloys resulted from the substitution Mm with La. The diffraction peak intensities of the (0 0 2) crystal planes of the as-cast and quenched alloys change obviously with the increase of the amount of substitution Mm with La. This shows that substituting Mm with La has an influence on the crystal orientation in process of the alloy crystallizing. The lattice constants of the as-cast and quenched ($22\ m\ s^{-1}$) alloys were calculated from the diffraction peaks of (1 0 1), (1 1 0), (2 0 0), (1 1 1) and (0 0 2) crystal planes of the main phase of the alloys by a method of least squares, and cell volumes of the alloys were calculated with formula $V = a^2 c \sin 60^\circ$. The calculated results were listed in Table 1. It can be derived from Table 1 that the lattice constants and cell volumes of the alloys increase with increase of the amount of substituting Mm with La. The capacities of the as-cast and quenched alloys increasing with the increase of the amount of substituting Mm with La is mainly attributed to the increase of the lattice constants and cell volumes of the alloys resulted from the substituting Mm with La [17].

Table 1
Lattice constants and cell volumes of the main phase in the as-cast and quenched alloys

Alloy	Lattice constants				Cell volumes	
	a (Å)		c (Å)		V (Å)^3	
	As-cast	22 ($m\ s^{-1}$)	As-cast	22 ($m\ s^{-1}$)	As-cast	22 ($m\ s^{-1}$)
La_0	5.0197	5.0198	4.0839	4.0671	89.11	88.75
$La_{0.45}$	5.0298	5.0317	4.0854	4.0662	89.53	88.79
$La_{0.75}$	5.0430	5.0535	4.0869	4.0669	89.46	89.94
La_1	5.0835	5.0878	4.0874	4.0674	91.45	91.18

3.2.2. Microstructure morphology

The microstructure morphologies of the as-cast and quenched alloys were observed by S.E.M., and the results were illustrated in Figs. 5 and 6, respectively. It can be seen from Fig. 5 that the grains of the as-cast alloys are very coarse, and the composition homogeneity is very poor. The effect of substituting Mm with La on the morphologies of the as-cast alloys is obvious. The composition homogeneity of the as-cast alloys becomes worse with the increase of the amount of the substituting Mm with La. The rapid quenching leads to obvious change of the morphologies of the alloys (Fig. 6). Comparing with the morphologies of the as-cast alloys, the rapid quenching markedly refined the grains of the alloys and made the component distribution of the alloys more homogenous. And the rapid quenching led to the change of the grain morphologies of the alloys from dendrite crystal to directional crystal. A fact worthy of remarking is that the grains of the as-quenched alloys with the quenching rate of $10\ m\ s^{-1}$ obviously coarsen with the increase of the amount of the substituting Mm with La (Fig. 6). This indicates that the substituting Mm with La had an obvious influence on the nucleation and growth of the alloys in process of disequilibrium crystallizing. In addition, with the increase of the amount of substituting Mm with La, the crystalline orientations of columnar crystals in the as-quenched alloys changed obviously and the consistency of the orientations of the columnar grains decreased.

The microstructure morphologies of the as-quenched $La_{0.45}$ alloy with different quenching rates were observed

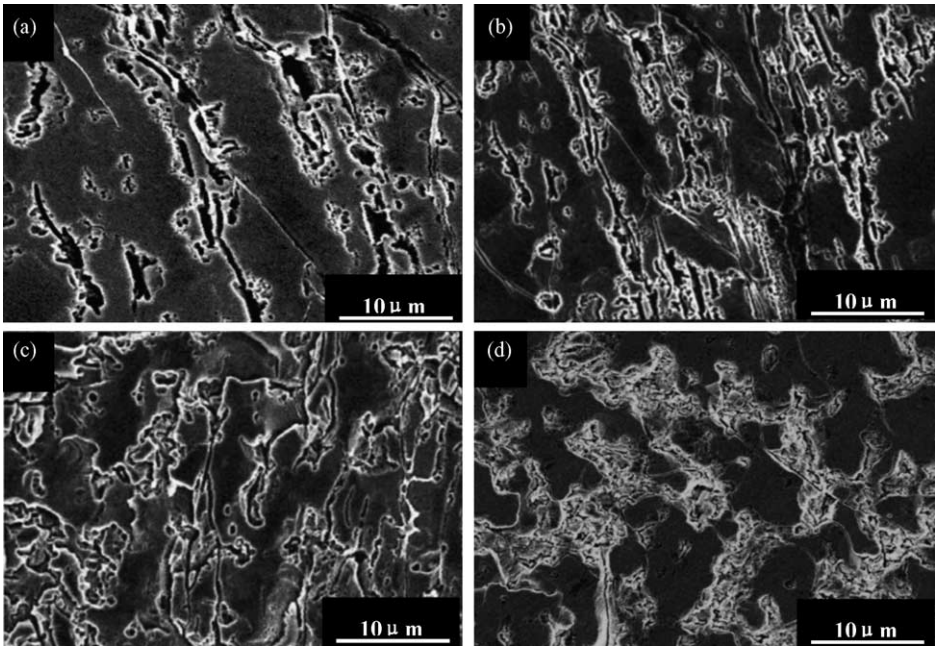

Fig. 5. The morphologies of the as-cast alloys (S.E.M.): (a) La_0; (b) $La_{0.45}$; (c) $La_{0.75}$; (d) La_1.

by TEM, and the crystal states of the alloy at the different quenching rates were analysed with selected area electron diffraction (SAD). The obtained results were illustrated in Fig. 7. It can be seen from Fig. 7 that the morphology and SAD of the as-quenched alloy with quenching rate of 16 m s^{-1} presented a microcrystalline structure, whereas a proper amount of amorphous phase formed in the as-quenched alloy with quenching rate of 28 m s^{-1}.

The above-mentioned results indicate that the substituting Mm with La led to an obvious change of the microstructures of the as-cast and quenched alloys and produced significant influences on the electrochemical performances of the alloys. Generally, the activation capacity of the hydrogen storage alloy is directly relevant to the change of the internal energy of the system before and after absorbing hydrogen. The larger the additive internal energy, which originates from oxidation

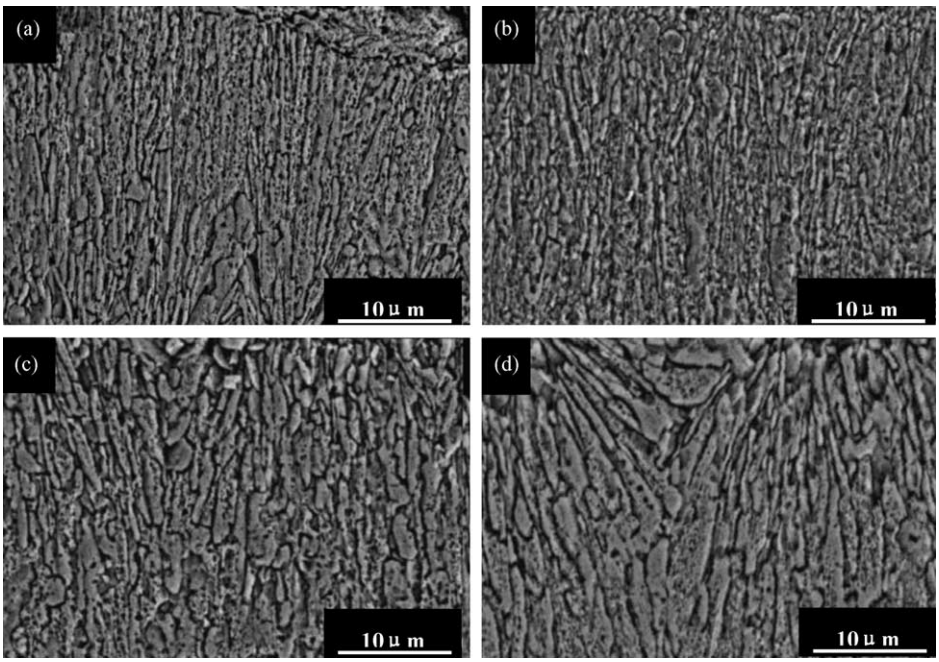

Fig. 6. The morphologies of the as-quenched (10 m s^{-1}) alloys (S.E.M.): (a) La_0; (b) $La_{0.45}$; (c) $La_{0.75}$; (d) La_1.

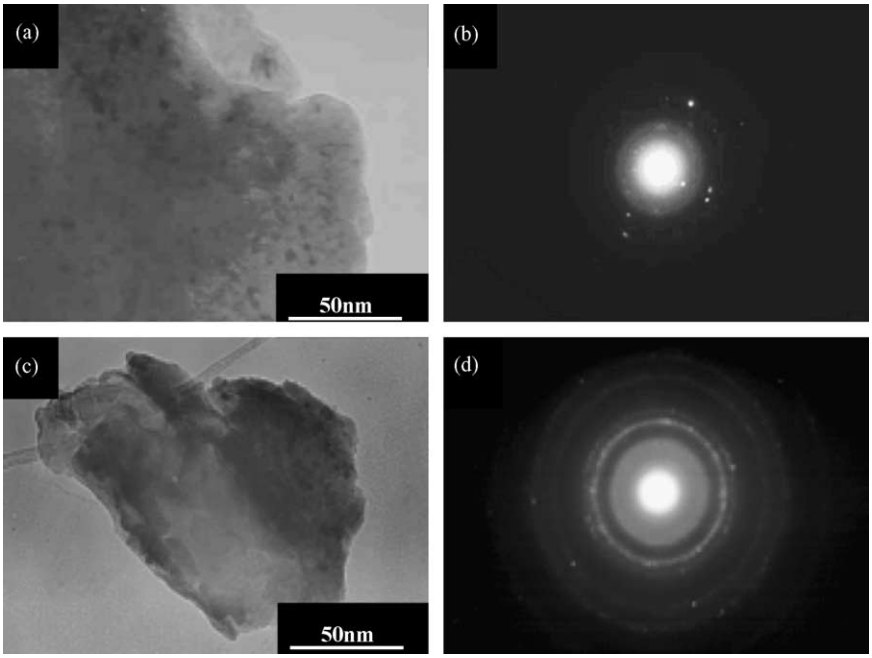

Fig. 7. The morphology and SAD of the as-quenched $La_{0.45}$ alloy taken by TEM: (a, b) morphology and SAD of the as-quenched alloy (16 m s^{-1}); (c, d) morphology and SAD of the as-quenched alloy (28 m s^{-1}).

film formed on the surface of the electrode alloy, and the strain energy, which is produced by hydrogen atom entering the interstitial of the tetrahedron or octahedron of the alloy lattice, the poorer is the activation performance of the alloy [18]. The results obtained by XRD show the lattice constants and cell volumes of the alloys increase with the increase of the amount of substitution Mm with La, and this enlarges the radiuses of the interstitial of the tetrahedron or octahedron of the lattice. And strain energy produced by hydrogen atoms entering the interstitials is small. Thus, the activation capability of the alloy can be enhanced. It is confirmed in the literature [19] that the main reason of the capacity decay of the electrode alloy is the pulverization and oxidation of the alloy in process of the charge–discharge cycle. The cycle stability of the alloy electrode mainly depends on the anti-pulverization and anti-corrosion capabilities of the alloys. The increase of the radius of the interstitials of the alloy produced by substituting Mm with La is favourable for the anti-pulverization capability of the alloy. The larger the radius of the interstitials of the lattice, the smaller strain energy produced by hydrogen atom entering the interstitial of the lattice, and the longer the cycle life of the alloy. The increase of La content decreases the anti-oxidation capability of the alloy. Therefore, the general effect of substituting Mm with La on the electrochemical cycle stabilities of the as-cast alloys is insignificant. The cause of substituting Mm with La decreasing the cycle lives of the as-quenched alloy is that the substituting Mm with La leads to the grains of the as-quenched alloys coarsen (Fig. 7) and the anti-pulverization capability of the alloys decreased. A typical structure composed of microcrystalline and amorphous phase, which is a decisive factor of the anti-pulverization capability of the alloys, exists in the as-quenched alloy with the quenching rate of 28 m s^{-1} (Fig. 7). Therefore, the substituting Mm with La has an insignificant influence on the cycle lives of the as-quenched alloys when the quenching is more than 22 m s^{-1} (Fig. 3).

3.3. Conclusions

1. The rare-earth-based Co-free AB_5-type $La_xMm_{1-x}(NiMnSiAlFe)_{4.9}$ (x = 0, 0.45, 0.75, 1.0) hydrogen storage alloys have a two-phase structure composed of a $CaCu_5$-type main phase and a small amount of Ce_2Ni_7-type secondary phase. The presence of the Ce_2Ni_7 phase is because the components of the alloys are non-stoichiometric. The Ce_2Ni_7-type phase decreases with the increase of the amount of La substitution. The substituting Mm with La leads to the obvious change of the diffraction peak intensities of the alloys and the increase of the lattice constants and cell volumes of the alloys.
2. The effect of the substituting Mm with La on the activation capabilities of the as-cast and quenched alloys is insignificant, but that on the capacities of the as-cast and quenched alloys is notable. The capacities of the as-cast and quenched alloys increase significantly with the increase of the amount of the La substitution. When the amount of the La substitution x increases from 0 to 1, the maximum capacity of the as-cast alloys with a current density of 60 mA g^{-1} increases from 273.45 to 304.47 mAh g^{-1}, and the that of the as-quenched alloys with a quenching rate of 10 m s^{-1} increases from 236.83 to 300.31 mAh g^{-1}.

3. The increase of the amount of the La substitution has an insignificant influence on the cycle lives of the as-cast and quenched alloys with the quenching rates of more than 22 m s^{-1}, but its influences on the cycle lives of as-quenched alloys with quenching rates of 10 and 16 m s^{-1} are very notable. When the amount of the La substitution x increases from 0 to 1, the capacity retaining rate of the as-cast alloys increases from 59.16 to 59.86%, and that of the as-quenched alloys with the quenching rate of 28 m s^{-1} decreases from 77.78 to 74.90%, whereas the capacity retaining rates of the as-quenched alloys with the quenching rate of 10 and 16 m s^{-1} decrease from 78.69 to 62.29 and 83.92 to 64.97%, respectively. One of the main reasons of the substituting Mm with La decreasing the cycle lives of the as-quenched alloys is that the increase of the amount of the substituting Mm with La leads to the grains of the as-quenched alloys coarsen.

Acknowledgements

This work is supported by National Natural Science Foundations of China (50131040 and 50071050).

References

[1] J.M. Cocciantelli, P. Bernard, S. Fernandez, J. Atkin, J. Alloys Compd. (1997) 253–254.
[2] P. Li, Y.-H. Zhang, X.-L. Wang, Y.-F. Lin, X.-H. Qu, J. Power Sources 124 (2003) 285.
[3] W.-K. Hu, J. Alloys Compd. 279 (1998) 295.
[4] P. Li, X.-L. Wang, Y.-H. Zhang, J.-M. Wu, R. Li, X.-H. Qu, J. Alloys Compd. 354 (2003) 310.
[5] W.-K. Hu, D.-M. Kim, K.-J. Jang, J.-Y. Lee, J. Alloys Compd. 269 (1998) 254.
[6] P. Li, X.-L. Wang, Y.-H. Zhang, R. Li, J.-M. Wu, X.-H. Qu, J. Alloys Compd. 353 (2003) 278.
[7] W.-K. Hu, H. Lee, D.-M. Kim, S.-W. Jeon, J.-Y. Lee, J. Alloys Compd. 268 (1998) 261.
[8] W.-K. Hu, J. Alloys Compd. 289 (1999) 299.
[9] D. Chartouni, F. Meli, A. Züttel, K. Gross, L. Schlapbach, J. Alloys Compd. 241 (1996) 160.
[10] K. Yashda, J. Alloys Compd. 253–254 (1997) 621.
[11] A. Zuttel, D. Chartouni, K. Gross, P. Spatz, M. Bachler, F. Lichtenberg, A. Folzer, N.J.E. Adkins, J. Alloys Compd. 253–254 (1997) 626.
[12] N. Higashiyama, Y. Mastuura, H. Nakamura, M. Kimoto, M. Nogami, I. Yonezu, K. Nishio, J. Alloys Compd. 253–254 (1997) 648.
[13] G.D. Adzic, J.R. Johnson, S. Mukerjee, J. McBreen, J.J. Reilly, J. Alloys Compd. 253–254 (1997) 579.
[14] T. Sakai, H. Miyamura, N. Kuriyama, H. Ishikawa, I. Uehara, Z. Phys. Chem. 183 (1994) 333.
[15] C. Li, X. Wang, X. Li, C. Wang, Electrochem. Acta 43 (1998) 1839.
[16] C. Li, X. Wang, X. Li, C. Wang, Acta Metall. Sinica 34 (3) (1998) 288.
[17] Q. Li, Y. Chen, M. Tu, G. Sang, M. Han, N. Li, D. Tang, Chin. J. Power Sources 24 (4) (2000) 246.
[18] Y. Zhou, Y. Lei, Y. Luo, S. Cheng, Q. Wang, Acta Metall. Sinica 32 (8) (1996) 857.
[19] Y. Li, Y.T. Cheng, J. Alloys Compd. 223 (1995) 6.